

On-line Approximation Based Aircraft Longitudinal Control

Jay Farrell[†], Manu Sharma[‡], and Marios Polycarpou[§]

[‡] Department of Electrical Engineering, University of California, Riverside, CA 92521

[§] Barron Associates, Inc., 1160 Pepsi Place, Suite 300, Charlottesville, Virginia 22901

[†] Dept. of Elect. and Comp. Eng. and Computer Science, U. of Cincinnati, OH 45221

Abstract

This document derives stable on-line approximation based control algorithms for application to the longitudinal control (γ, α, Q, V) for an uninhabited combat air vehicle (UCAV). The objectives of the control approach are to stabilize the aircraft dynamics and achieve accurate command tracking in the presence of significant nonlinear model error. This error could be due to decreased modeling effort during the design process or the result of events that occur during the vehicle flight (i.e., battle damage). Lyapunov stability analysis and simulation demonstrations of the achieved performance are included.

1 Introduction

The past few decades have witnessed the development of a number of nonlinear control methodologies for application to advanced flight vehicles. Offering both increases in performance as well as reduced development times by dealing with the complete dynamics of the vehicle rather than point designs, nonlinear control tools provide a great deal of design flexibility. Feedback linearization, in its various forms, is perhaps the most commonly employed nonlinear control method in this arena [1, 5, 11, 13, 14, 19]. In addition to feedback linearization, other nonlinear methods have also been investigated for flight control. Reference [2] presents a nonlinear model predictive control approach that relies on a Taylor series approximation to the system's differential equations. Optimal control techniques are applied to control load-factor in [10]. Prelinearization theory and singular perturbation theory are applied for the derivation of inner and outer loop controllers in [13].

The main drawback to the nonlinear control approaches mentioned above is that, as model-based control methods, they require accurate knowledge of the plant dynamics. This is of significance in flight control since aerodynamic parameters always contain some degree of uncertainty. Although, some of these approaches are robust to small modeling errors, they are not intended to accommodate significant unanticipated errors that can

occur in the event of failure or battle damage. In such an event, the aerodynamics can change rapidly and deviate significantly from the model used for control design. UCAV's are particularly susceptible to such events since there is no pilot onboard.

Various direct and indirect adaptive approaches have been proposed to address circumstances in which significant modeling error is present. For example, the indirect model predictive method of [25] was successfully demonstrated in flight on the VISTA F-16. However, proofs of stability for these indirect linear adaptive controllers have not been presented. Adaptive backstepping type approaches, in which the aircraft model parameters are estimated on-line, have also been explored for flight control [18, 21]. These methods allow a total stability analysis, but do not provide an easy means of designing the transient response [21]. In addition, since the approach is based on estimated linearized aircraft model parameters, changes in operating point can generate significant tracking error transients while the new linearized model parameters are being estimated. Direct adaptive control approaches that have been successfully demonstrated in flight are provided in [4, 7, 17].

This article presents a flight-control approach that is based on ideas from feedback linearization and backstepping [12]. The control law incorporates on-line function-approximators to estimate aerodynamic force and moment functions using the theory for approximation based nonlinear control, e.g. [8, 9, 15, 16]. The main advantages of this approach include: the controller has a small number of control parameters that are straightforward to select; the control law automatically adjusts itself to accommodate changes to the aerodynamic properties of the vehicle; a complete proof of stability is included; and, analysis of the effects of model errors is facilitated. The main motivations for this work were: to produce a simplified control design that is robust to model error, to accommodate large changes in the vehicle dynamics (e.g. damage) on-line, and to *learn* the aerodynamic functions for the vehicle. An anticipated benefit from these properties is that the controller could

be applied to an aircraft that it was not explicitly designed for, e.g. an aircraft of the same family but different configuration. Additionally, the controller could be developed using a lower fidelity model than required by current methods, thereby offering a cost savings. This control method is expected to provide significant reduction in design time since the control system design does not depend on a conglomeration of point designs. Reference [20] discusses some of these benefits in the context of adaptive control for guided munitions.

The approach herein develops *on-line* approximations to the aircraft force and moment functions. Such *off-line* approximations have a long history in the aerodynamics community. Trankle reviews off-line system identification methods in [24]. The example of this article will use splines in the system identification process. An overview, with several examples, of off-line, spline based, system identification based on data partitioning is presented in [3]. Finally, the article [23] performs off-line estimation of additive functional corrections to the aircraft model. The corrections are multidimensional cubic splines (see p. 1294), which is interesting relative to the approach herein where such model error is approximated on-line.

2 Outer Loop Control Derivation

This section presents an on-line approximation based approach to achieve ‘asymptotic perfect tracking’ for the flight path angle γ and speed V^1 . Control of γ is achieved through the intermediate variables α and Q . The controller will force α and Q to track the internally generated signals α_c and Q_c . In this approach, we assume that the aerodynamic drag and lift forces and pitch moment are not known *a priori*. We approximate the drag and lift forces and pitch moment functions on-line and use the approximated functions in a backstepping controller.

2.1 Control of (γ, α, Q)

The flight path angle is defined as (see p. 88, 131 in [22])

$$\gamma \equiv \sin^{-1} \left(\frac{\dot{h}}{V} \right).$$

The longitudinal model (see Appendix A), valid for small sideslip and roll angles, has $\gamma = \theta - \alpha$ with dynamics

$$\begin{aligned} \dot{\gamma} &= \frac{L}{mV} + \left[\frac{T \sin(\alpha) - mg \cos(\gamma)}{mV} \right] \\ &= \frac{L}{mV} + f_\gamma(\alpha, T, V) \end{aligned}$$

where $f_\gamma = \left[\frac{T \sin(\alpha) - mg \cos(\gamma)}{mV} \right]$ is a known function. Therefore, we have the following four dynamic equations, but only three independent variables:

$$\begin{aligned} \dot{\gamma} &= \frac{L}{mV} + f_\gamma & \dot{\alpha} &= -\frac{L}{mV} + Q - f_\gamma \\ \dot{\theta} &= Q & \dot{Q} &= c_7 \bar{M} + f_Q \end{aligned}$$

where f_Q is a known function due to inertial coupling. To control γ through backstepping, the designer can choose either α or θ as an intermediate variable. Subsection 2.1.1 presents a back-stepping based approach for the control of (γ, α, Q) . A controller using θ as the intermediate variable can be similarly derived.

2.1.1 Backstepping control of (γ, α, Q) : We will work with the standard aircraft ‘coefficient’ notation [22] by letting

$$\begin{aligned} L(x) &= \bar{q}S(C_L(x_r) + C_{L_\alpha}(x_r)) + \epsilon_{L_1}(x) \\ \bar{M}(x) &= \bar{q}S\bar{c} \left(C_{M_o}(x_r) + C_{M_Q}(x_r) \frac{\bar{c}Q}{2V} \right. \\ &\quad \left. + \sum_{i=1}^m C_{M_{\delta_i}}(x_r) \delta_i \right) + \epsilon_{M_1}(x). \end{aligned}$$

The $(m+4)$ nondimensional ‘coefficient’ functions C_{M_o} , C_{M_Q} , C_L , C_{L_α} , and $C_{M_{\delta_i}}$ are sufficient to illustrate the method. The main assumption is that ϵ_{M_1} and ϵ_{L_1} are small for x in the operating envelope \mathcal{D} . Additional coefficients may be required depending on the characteristics of the aircraft to be controlled, but these are sufficient to model the aerodynamics of most aircraft. The vector variable x_r represents the subset of the vehicle state, operating point, and control vector information that dominates the functional dependence of the lift function. This is clarified further in the example of Section 3.

The (γ, α, Q) dynamic equations are

$$\begin{aligned} \dot{\gamma} &= \frac{\bar{q}S(C_L + C_{L_\alpha}\alpha)}{mV} + f_\gamma + \frac{\epsilon_{L_1}}{mV} \\ \dot{\alpha} &= -\frac{\bar{q}S(C_L + C_{L_\alpha}\alpha)}{mV} + Q - f_\gamma - \frac{\epsilon_{L_1}}{mV} \\ \dot{Q} &= f_Q + c_7 \left[\bar{q}S\bar{c} \left(C_{M_o} + C_{M_Q} \frac{\bar{c}Q}{2V} \right) + u_Q + \epsilon_{M_1} \right] \end{aligned}$$

where $G_Q(x_r) = \bar{q}S\bar{c} [C_{M_{\delta_1}}(x_r), \dots, C_{M_{\delta_m}}(x_r)]$, $u_Q = G_Q(x_r)\delta$, and (x_r) has been dropped to reduce the complexity of the notation. Assume that $(\gamma_c, \dot{\gamma}_c)$ are bounded and available. The variables (α_c, Q_c) will be defined below. The dynamic equations for the tracking errors $\tilde{\gamma} = (\gamma - \gamma_c)$, $\tilde{\alpha} = (\alpha - \alpha_c)$, and $\tilde{Q} = (Q - Q_c)$

¹Due to space limitations, the derivation of the velocity controller is not included herein. It is used in the simulation example. Its derivation is parallel to the derivations herein.

are

$$\begin{aligned}\dot{\gamma} &= \frac{\bar{q}S(C_L + C_{L\alpha}(\alpha_c + \tilde{\alpha}))}{mV} + f_\gamma - \dot{\gamma}_c + \frac{\epsilon_{L_1}}{mV} \\ \dot{\alpha} &= -\frac{\bar{q}S(C_L + C_{L\alpha}\alpha)}{mV} + Q_c + \tilde{Q} - f_\gamma - \dot{\alpha}_c - \frac{\epsilon_{L_1}}{mV} \\ \dot{Q} &= c_7 \left(\bar{q}S\bar{c} \left(C_{M_o} + C_{M_Q} \frac{\bar{c}Q}{2V} \right) + u_Q + \epsilon_{M_1} \right) + f_Q - \dot{Q}_c\end{aligned}$$

Known Aerodynamic Functions. In the case where the lift and moment functions are known, the backstepping control signals can be selected as follows. For the γ dynamics, select

$$\alpha_c = \frac{1}{C_{L\alpha}} \left(-C_L + \frac{mV}{\bar{q}S} (-f_\gamma + \dot{\gamma}_c - K_\gamma \tilde{\gamma} + \nu_\gamma) \right) \quad (1)$$

where ν_γ is a term that will be defined later to ensure robustness to modeling errors. Then, the controlled γ tracking error dynamics are

$$\dot{\tilde{\gamma}} = -K_\gamma \tilde{\gamma} + \nu_\gamma + \tilde{\alpha} \frac{\bar{q}S C_{L\alpha}}{mV} + \frac{\epsilon_{L_1}}{mV}. \quad (2)$$

For the α dynamics, select

$$Q_c = \frac{\bar{q}S(C_L + C_{L\alpha}\alpha)}{mV} - K_\alpha \tilde{\alpha} + f_\gamma + \dot{\alpha}_c + \nu_\alpha - \tilde{\gamma} \frac{\bar{q}S C_{L\alpha}}{mV}$$

where $\dot{\alpha}_c$ is an approximation to $\dot{\alpha}$ (e.g., $\dot{\alpha}_c = \frac{s}{\tau_\alpha s + 1} \alpha_c$)². Then the controlled α tracking error dynamics are

$$\dot{\tilde{\alpha}} = -K_\alpha \tilde{\alpha} + \nu_\alpha + \tilde{Q} + (\dot{\alpha}_c - \dot{\alpha}) - \tilde{\gamma} \frac{\bar{q}S C_{L\alpha}}{mV} - \frac{\epsilon_{L_1}}{mV}.$$

For the Q dynamics, select

$$\begin{aligned}u_Q &= -\bar{q}S\bar{c} \left(C_{M_o} + C_{M_Q} \frac{\bar{c}Q}{2V} \right) \\ &\quad + \frac{-K_Q \tilde{Q} + \nu_Q - \tilde{\alpha} + \dot{Q}_c - f_Q}{c_7}\end{aligned}$$

where \dot{Q}_c is an approximation to \dot{Q} (e.g., $\dot{Q}_c = \frac{s}{\tau_Q s + 1} Q_c$ see the comments for $\dot{\alpha}_c$). Then the controlled Q tracking error dynamics are

$$\dot{\tilde{Q}} = -K_Q \tilde{Q} + (\dot{Q}_c - \dot{Q}) + \nu_Q - \tilde{\alpha} + c_7 \epsilon_{M_1}.$$

²At least three approaches to handle the term $\dot{\alpha}_c$ are possible: 1) Compute $\dot{\alpha}_c$ exactly – This is complex and requires knowledge of $\dot{\alpha}$ which is not generally available directly. 2) Neglect $\dot{\alpha}_c$ completely – This would require increasing $\bar{\epsilon}$ enough to over bound the entire derivative. 3) Use a filtered version of the derivative in place of the derivative – In this case, $\bar{\epsilon}$ only is increased by the error between the derivative and the filtered derivative. The presentation to follow applies to any of these choices, but the authors favor method 3 and use it in the example. Method 3 works well, because the signal that is being filtered is continuous. Therefore, the signal energy is at low frequencies where the specified filter is a good approximation to the derivative. Note that this is by design since the designer selects the bandwidth of the derivative filter (i.e., $\frac{1}{\tau_\alpha}$) and the bandwidth of α_c (i.e., K_γ).

At this point, Lyapunov analysis could prove a result similar to Theorem 2.1 (proved later in this article); however, since this is only an intermediate result and we have limited space, we do not do so. Note that for a well-modeled system each of the terms $\frac{\epsilon_{L_1}}{mV}$, $(\dot{\alpha}_c - \dot{\alpha} - \frac{\epsilon_{L_1}}{mV})$, $(\dot{Q}_c - \dot{Q} + c_7 \epsilon_{M_1})$ would be quite small; however, modeling error, possibly due to in-flight changes in the aircraft, will excite tracking error to possibly unacceptable limits. The challenge, as addressed in the next section is to ensure that the system is well modeled, even when in-flight events change the vehicle dynamics. This will be achieved without resorting to high control gains.

Unknown Aerodynamic Functions. The previous design and analysis was based on exact knowledge of the coefficient functions. Now, we consider the case where the functions C_L , $C_{L\alpha}$, C_{M_o} , C_{M_Q} , and $C_{M_{\delta_i}}$ are unknown and are approximated on-line. Their on-line approximations are given by

$$\begin{aligned}\hat{C}_L(x_r) &= \theta_{C_L}^T \phi(x_r), & \hat{C}_{L\alpha}(x_r) &= \theta_{C_{L\alpha}}^T \phi(x_r), \\ \hat{C}_{M_o}(x_r) &= \theta_{M_o}^T \phi(x_r), & \hat{C}_{M_Q}(x_r) &= \theta_{M_Q}^T \phi(x_r), \\ \hat{C}_{M_{\delta_i}}(x_r) &= \theta_{M_{\delta_i}}^T \phi(x_r) & i &= 1, \dots, m.\end{aligned}$$

where $x_r \in \mathbb{R}^d$ and $\phi(x_r) : \mathbb{R}^d \mapsto \mathbb{R}^N$ is a regressor vector containing the basis functions for the approximation.

Denote the operating envelope by \mathcal{D} , which is assumed to be compact (i.e., closed and bounded). Then for continuous $\bar{M}(x_r)$, there exists a parameter matrix

$$\begin{aligned}\Theta_M^* &= \underset{\Theta_M}{\operatorname{argmin}} [\sup_{\mathcal{D}} |\bar{M}(x_r) - \\ &\quad \bar{q}S\bar{c} \left(\theta_{M_o}^T + \theta_{M_Q}^T \frac{\bar{c}Q}{2V} + \sum_{i=1}^m \theta_{M_{\delta_i}}^T \delta_i \right) \phi(x_r)|].\end{aligned}$$

In addition, there exists an upper bound $\bar{\epsilon}_{M_2}$ such that

$$\sup_{\mathcal{D}} |\epsilon_{M_2}(x_r)| = \bar{\epsilon}_{M_2} < \infty, \text{ where}$$

$$\begin{aligned}\epsilon_{M_2}(x_r) &= \bar{M}(x_r) - \bar{q}S\bar{c} \left(\theta_{M_o}^T + \theta_{M_Q}^T \frac{\bar{c}Q}{2V} \right. \\ &\quad \left. + \sum_{i=1}^m \theta_{M_{\delta_i}}^T \delta_i \right) \Big|_{\Theta_M^*} \phi(x_r)\end{aligned}$$

and $\Theta_M = [\theta_{M_o}, \theta_{M_Q}, \theta_{M_{\delta_1}}, \dots, \theta_{M_{\delta_m}}] \in \mathbb{R}^{N \times (2+m)}$. Since the designer has the freedom to choose the basis set $\phi(\cdot)$, the basis set can be selected so that $\bar{\epsilon}_{M_2}$ is small. It is important to note that the values of Θ_M^* and $\bar{\epsilon}_{M_2}$ need not be known and these quantities are not used in the control calculations. It is sufficient to know that these quantities exist.

Two model error terms have been introduced. The term ϵ_{M_1} denotes the error incurred by neglecting some of the state variables in the model representation of the moment. This error could be reduced by including additional input variables in the moment model or by including additional aerodynamic coefficients. The term ϵ_{M_2} denotes the approximation error incurred due to the choice of the approximator basis set. This error can be reduced by the increasing the number of basis elements. There is an inherent tradeoff. Reduction of either error will require additional computation. Therefore, the regression vector and the dimension of the input space must be selected judiciously. Note also, that the on-line approximation $\hat{M}(x_r)$ only achieves the approximation error ϵ_{M_2} asymptotically if Θ_M converges to Θ_M^* .

By analysis similar to that related to ϵ_{M_2} , we define

$$\begin{aligned}\Theta_L^* &= \underset{\Theta_L}{\operatorname{argmin}} \left[\sup_{x_r \in \mathcal{D}} |(C_L(x_r) + C_{L_\alpha}(x_r)\alpha) \right. \\ &\quad \left. - (\theta_{C_L}^T + \theta_{C_{L_\alpha}}^T \alpha) \phi(x_r) \right] \\ \epsilon_{L_2}(x_r) &= C_L(x_r) + C_{L_\alpha}(x_r)\alpha - (\theta_{C_L}^T + \theta_{C_{L_\alpha}}^T \alpha) \Big|_{\Theta_L^*} \phi(x_r) \\ \bar{\epsilon}_{L_2} &= \sup_{x_r \in \mathcal{D}} |\epsilon_{L_2}(x_r)|\end{aligned}$$

where $\Theta_L = [\theta_{C_L}; \theta_{C_{L_\alpha}}]$. The bound $\bar{\epsilon}_{L_2}$ is well-defined and small for appropriate selection of the basis vector $\phi(x_r)$. Therefore,

$$(C_L(x_r) + C_{L_\alpha}(x_r)\alpha) = (\theta_{C_L}^T \phi(x_r) + \theta_{C_{L_\alpha}}^T \phi(x_r)\alpha) - (\tilde{\theta}_{C_L}^T \phi(x_r) + \tilde{\theta}_{C_{L_\alpha}}^T \phi(x_r)\alpha) + \epsilon_{L_2}(x_r) \quad (3)$$

where $\tilde{\theta}_{C_L} = \theta_{C_L} - \theta_{C_L}^*$ and $\tilde{\theta}_{C_{L_\alpha}} = \theta_{C_{L_\alpha}} - \theta_{C_{L_\alpha}}^*$. Note that $\theta_{C_L}^*$, $\theta_{C_{L_\alpha}}^*$, and $\epsilon_{L_2}(x_r)$ are used only for analysis and are not needed for control law implementation.

For the γ dynamics replace the unknown functions by their approximations in the selection of the control law

$$\alpha_c = \frac{1}{\hat{C}_{L_\alpha}} \left(-\hat{C}_L + \frac{mV}{\bar{q}S} (-f_\gamma + \dot{\gamma}_c - K_\gamma \tilde{\gamma} + \nu_\gamma) \right). \quad (4)$$

Then, the controlled γ tracking error dynamics are

$$\begin{aligned}\dot{\tilde{\gamma}} &= -K_\gamma \tilde{\gamma} + \nu_\gamma + \tilde{\alpha} \frac{\bar{q}S \hat{C}_{L_\alpha}}{mV} \\ &\quad - \frac{\bar{q}S}{mV} \left(\tilde{\theta}_{C_L}^T \phi + \tilde{\theta}_{L_\alpha}^T \phi \alpha \right) + \frac{(\epsilon_{L_1} + \bar{q}S \epsilon_{L_2})}{mV}.\end{aligned}$$

Define the γ Lyapunov function as

$$\mathcal{V}_\gamma = \frac{1}{2} \tilde{\gamma}^2 + \frac{1}{2} \left(\tilde{\theta}_{C_L}^T \Gamma_{C_L}^{-1} \tilde{\theta}_{C_L} + \tilde{\theta}_{C_{L_\alpha}}^T \Gamma_{C_{L_\alpha}}^{-1} \tilde{\theta}_{C_{L_\alpha}} \right)$$

where throughout this article the subscripted Γ symbols are positive definite parameter adaptation gains.

The derivative of \mathcal{V}_γ along solutions of the $\tilde{\gamma}$ dynamic equation is

$$\begin{aligned}\dot{\mathcal{V}}_\gamma &= -K_\gamma \tilde{\gamma}^2 + \nu_\gamma \tilde{\gamma} + \tilde{\gamma} \tilde{\alpha} \frac{\bar{q}S \hat{C}_{L_\alpha}}{mV} + \tilde{\gamma} \frac{(\epsilon_{L_1} + \bar{q}S \epsilon_{L_2})}{mV} \\ &\quad + \tilde{\theta}_{C_L}^T \Gamma_{C_L}^{-1} \left(\dot{\theta}_{C_L} - \Gamma_{C_L} \frac{\bar{q}S}{mV} \phi \tilde{\gamma} \right) \\ &\quad + \tilde{\theta}_{C_{L_\alpha}}^T \Gamma_{C_{L_\alpha}}^{-1} \left(\dot{\theta}_{C_{L_\alpha}} - \Gamma_{C_{L_\alpha}} \frac{\bar{q}S}{mV} \phi \alpha \tilde{\gamma} \right).\end{aligned}$$

Since the unknown functions C_L and C_{L_α} also appear in α dynamics, we delay the selection of the update laws for θ_{C_L} and $\theta_{C_{L_\alpha}}$ until the next step of the backstepping procedure. For the α dynamics, select

$$Q_c = \frac{\bar{q}S (\hat{C}_L + \hat{C}_{L_\alpha} \alpha)}{mV} - K_\alpha \tilde{\alpha} - f_\alpha + \dot{\alpha}_c + \nu_\alpha - \tilde{\gamma} \frac{\bar{q}S \hat{C}_{L_\alpha}}{mV} \quad (5)$$

Based on the above control law, the controlled α tracking error dynamics are

$$\begin{aligned}\dot{\tilde{\alpha}} &= -K_\alpha \tilde{\alpha} + \nu_\alpha + \tilde{Q} - \tilde{\gamma} \frac{\bar{q}S \hat{C}_{L_\alpha}}{mV} + \\ &\quad \frac{\bar{q}S}{mV} \left(\tilde{\theta}_{C_L}^T \phi + \tilde{\theta}_{L_\alpha}^T \phi \alpha \right) - \frac{(\epsilon_{L_1} + \bar{q}S \epsilon_{L_2})}{mV} + (\dot{\alpha}_c - \dot{\alpha}_c).\end{aligned}$$

Define the (γ, α) Lyapunov function as

$$\mathcal{V}_{(\gamma, \alpha)} = \mathcal{V}_\gamma + \frac{1}{2} \tilde{\alpha}^2.$$

The derivative of $\mathcal{V}_{(\gamma, \alpha)}$ along solutions of the $(\tilde{\gamma}, \tilde{\alpha})$ dynamic equations is (after simplification)

$$\begin{aligned}\dot{\mathcal{V}}_{(\gamma, \alpha)} &= -(K_\gamma \tilde{\gamma}^2 + K_\alpha \tilde{\alpha}^2) + \tilde{Q} \tilde{\alpha} + \nu_\gamma \tilde{\gamma} + \nu_\alpha \tilde{\alpha} \\ &\quad + \tilde{\alpha} (\dot{\alpha}_c - \alpha_c) + (\tilde{\gamma} - \tilde{\alpha}) \frac{(\epsilon_{L_1} + \bar{q}S \epsilon_{L_2})}{mV} \\ &\quad + \tilde{\theta}_{C_L}^T \Gamma_{C_L}^{-1} \left(\dot{\theta}_{C_L} - \Gamma_{C_L} \frac{\bar{q}S}{mV} \phi (\tilde{\gamma} - \tilde{\alpha}) \right) \\ &\quad + \tilde{\theta}_{C_{L_\alpha}}^T \Gamma_{C_{L_\alpha}}^{-1} \left(\dot{\theta}_{C_{L_\alpha}} - \Gamma_{C_{L_\alpha}} \frac{\bar{q}S \tilde{\alpha}}{mV} \phi \alpha (\tilde{\gamma} - \tilde{\alpha}) \right).\end{aligned}$$

Based on the above Lyapunov function derivative, we now select the adaptive laws for θ_{C_L} and $\theta_{C_{L_\alpha}}$:

$$\dot{\theta}_{C_L} = \Gamma_{C_L} \frac{\bar{q}S}{mV} \phi (\tilde{\gamma} - \tilde{\alpha}) \quad (6)$$

$$\dot{\theta}_{C_{L_\alpha}} = \Gamma_{C_{L_\alpha}} \frac{\bar{q}S}{mV} \phi \alpha (\tilde{\gamma} - \tilde{\alpha}) \quad (7)$$

for $|\tilde{\gamma}| > \left| \frac{1}{K_\gamma} \frac{(\epsilon_{L_1} + \bar{q}S \epsilon_{L_2})}{mV} \right|$ and

$$|\tilde{\alpha}| > \left| \frac{1}{K_\alpha} \left[(\dot{\alpha}_c - \alpha_c) + \frac{(\epsilon_{L_1} + \bar{q}S \epsilon_{L_2})}{mV} \right] \right|.$$

For the Q dynamics, select

$$\begin{aligned}u_Q &= -\bar{q}S \bar{c} \left(\hat{C}_{M_o} + \hat{C}_{M_Q} \frac{\bar{c}Q}{2V} \right) \\ &\quad + \frac{-K_Q \tilde{Q} + \nu_Q - \tilde{\alpha} + \dot{Q}_c - f_Q}{c_7}.\end{aligned}$$

Then the controlled Q tracking error dynamics are

$$\begin{aligned} \dot{\tilde{Q}} &= -K_Q \tilde{Q} + \nu_Q - \tilde{\alpha} + c_7 [\epsilon_{M_2} + \epsilon_{M_1}] + (\dot{\tilde{Q}}_c - \dot{Q}_c) \\ &\quad + c_7 \bar{q} S \bar{c} \left[\left(\tilde{\theta}_{M_o}^T + \tilde{\theta}_{M_Q}^T \frac{\bar{c} Q}{2V} + \sum_{i=1}^m \tilde{\theta}_{M_{\delta_i}}^T \delta_i \right) \phi \right]. \end{aligned}$$

Define the (γ, α, Q) Lyapunov function as

$$\begin{aligned} \mathcal{V}_{(\gamma, \alpha, Q)} &= \mathcal{V}_{(\gamma, \alpha)} + \frac{1}{2} \tilde{Q}^2 + \\ &\quad \frac{1}{\mu} \left[\tilde{\theta}_{M_o}^T \Gamma_{M_o}^{-1} \tilde{\theta}_{M_o} + \tilde{\theta}_{M_Q}^T \Gamma_{M_Q}^{-1} \tilde{\theta}_{M_Q} + \sum_{i=1}^m \tilde{\theta}_{M_{\delta_i}}^T \Gamma_{M_{\delta_i}}^{-1} \tilde{\theta}_{M_{\delta_i}} \right]. \end{aligned}$$

The derivative of $\mathcal{V}_{(\gamma, \alpha, Q)}$ along solutions of the (γ, α, Q) tracking error dynamic equations with the moment coefficient update laws defined by

$$\dot{\tilde{\theta}}_{M_o} = \mu c_7 (\bar{q} S \bar{c}) \tilde{Q} \Gamma_{M_o} \phi(x_r) \quad (8)$$

$$\dot{\tilde{\theta}}_{M_Q} = \mu c_7 (\bar{q} S \bar{c}) \tilde{Q} \Gamma_{M_Q} \phi(x_r) \frac{\bar{c} Q}{2V} \quad (9)$$

$$\dot{\tilde{\theta}}_{M_{\delta_i}} = \mu c_7 (\bar{q} S \bar{c}) \tilde{Q} \Gamma_{M_{\delta_i}} \phi(x_r) \delta_i, \quad (10)$$

for $i = 1, \dots, m$, with the deadzone

$$|K_Q \tilde{Q}| < \left| c_7 [\epsilon_{M_2} + \epsilon_{M_1}] + (\dot{\tilde{Q}}_c - \dot{Q}_c) \right|$$

is (after simplification)

$$\begin{aligned} \dot{\mathcal{V}}_{(\gamma, \alpha, Q)} &= - \left(K_\gamma \tilde{\gamma}^2 + K_\alpha \tilde{\alpha}^2 + K_Q \tilde{Q}^2 \right) \\ &\quad + \nu_\gamma \tilde{\gamma} + \nu_\alpha \tilde{\alpha} + \nu_Q \tilde{Q} + \epsilon \end{aligned}$$

where $\epsilon = \tilde{\alpha}(\dot{\tilde{\alpha}}_c - \dot{\alpha}_c) + (\tilde{\gamma} - \tilde{\alpha}) \frac{(\epsilon_{L_1} + \bar{q} S \epsilon_{L_2})}{mV} + c_7 [\epsilon_{M_2} + \epsilon_{M_1}] \tilde{Q} + (\dot{\tilde{Q}}_c - \dot{Q}_c) \tilde{Q}$. Therefore, for $(K_\gamma, K_\alpha, K_Q)$ positive:

1. If $(\dot{\tilde{\alpha}}_c - \dot{\alpha}_c) = (\dot{\tilde{Q}}_c - \dot{Q}_c) = \epsilon_{M_1} = \epsilon_{M_2} = \epsilon_{L_1} = \epsilon_{L_2} = 0$, then even for $\nu_\gamma = \nu_\alpha = \nu_Q = 0$ we have $\dot{\mathcal{V}}_{(\gamma, \alpha, Q)}$ negative definite, which implies (by Barbalat's Lemma) that the tracking error is asymptotically stable.
2. If ν_γ has sign opposite to $\tilde{\gamma}$ and magnitude larger than $\left| \frac{\epsilon_{L_1} + \bar{q} S \epsilon_{L_2}}{mV} \right|$, ν_α has sign opposite to $\tilde{\alpha}$ and magnitude greater than $\left| \dot{\tilde{\alpha}}_c - \dot{\alpha}_c - \frac{\epsilon_{L_1} + \bar{q} S \epsilon_{L_2}}{mV} \right|$, and ν_Q has sign opposite to \tilde{Q} and magnitude larger than $\left| \dot{\tilde{Q}}_c - \dot{Q}_c + c_7 (\epsilon_{M_1} + \epsilon_{M_2}) \right|$, then $\dot{\mathcal{V}}_{(\gamma, \alpha, Q)}$ is negative definite. Therefore, by Barbalat's Lemma, each tracking error is asymptotically stable.
3. If each of the terms $\frac{\epsilon_{L_1}}{mV}$, $\bar{q} S \frac{\epsilon_{L_2}}{mV}$, $(\dot{\tilde{\alpha}}_c - \dot{\alpha}_c)$, $(\dot{\tilde{Q}}_c - \dot{Q}_c)$, and $(c_7 (\epsilon_{M_1} + \epsilon_{M_2}))$ is bounded;

then the tracking error is uniformly ultimately bounded. Each of these terms should be small for a properly designed system. It can be shown that $\tilde{\gamma}$, $\tilde{\alpha}$, \tilde{Q} , $\tilde{\Theta}$, $\tilde{\Theta} \in \mathcal{L}_\infty$ and that the signals $\tilde{\gamma}$, $\tilde{\alpha}$, \tilde{Q} are each s^2 -small in the mean squared sense, where

$$\begin{aligned} s^2 &= \frac{1}{K_\gamma} \left(\frac{\epsilon_{L_1} + \bar{q} S \epsilon_{L_2}}{mV} \right)^2 \\ &\quad + \frac{1}{K_\alpha} \left(\dot{\tilde{\alpha}}_c - \dot{\alpha}_c - \frac{\epsilon_{L_1} + \bar{q} S \epsilon_{L_2}}{mV} \right)^2 \\ &\quad + \frac{1}{K_Q} \left(c_7 [\epsilon_{M_2} + \epsilon_{M_1}] + (\dot{\tilde{Q}}_c - \dot{Q}_c) \right)^2 \quad (11) \end{aligned}$$

If ν_γ has sign opposite to $\tilde{\gamma}$, ν_α has sign opposite to $\tilde{\alpha}$, and ν_Q has sign opposite to \tilde{Q} , then the magnitude of this bound is decreased.

The third case will be the case that holds in most applications. Although it is possible to decrease s^2 by increasing $(K_\gamma, K_\alpha, K_Q)$, this is not a desirable approach, since these parameters determine the closed loop bandwidth. Also, the designer can force the second case by selecting $\nu_\gamma = K_1 \text{sign}(\tilde{\gamma})$, $\nu_\alpha = K_2 \text{sign}(\tilde{\alpha})$, $\nu_Q = K_3 \text{sign}(\tilde{Q})$ with K_1, K_2, K_3 sufficiently large, but this will cause the control signals to be discontinuous, which is not desirable. Case three is preferred since s is small. The magnitude of s can be controlled by the designer through the specification of $\phi(x_r)$ and the choice of aerodynamic coefficients included in the model.

2.2 Control Law Summary

The equations of the on-line approximation based controller are summarized in Table 1. The properties of this controller are summarized in Theorem 2.1.

Theorem 2.1 *The control law summarized in Table 1 stabilizes the (γ, α, Q) dynamics of an aircraft in the sense that*

1. $(\tilde{\gamma}, \tilde{\alpha}, \tilde{Q})$ are each ultimately bounded by $|\tilde{\gamma}| \leq \left| \frac{1}{K_\gamma} \frac{(\epsilon_{L_1} + \bar{q} S \epsilon_{L_2})}{mV} \right|$, $|\tilde{\alpha}| \leq \left| \frac{1}{K_\alpha} \left[(\dot{\tilde{\alpha}}_c - \dot{\alpha}_c) + \frac{(\epsilon_{L_1} + \bar{q} S \epsilon_{L_2})}{mV} \right] \right|$, and $|K_Q \tilde{Q}| \leq \left| c_7 [\epsilon_{M_2} + \epsilon_{M_1}] + (\dot{\tilde{Q}}_c - \dot{Q}_c) \right|$;
2. $\tilde{\gamma}$, $\tilde{\alpha}$, \tilde{Q} , $\tilde{\Theta}$, $\dot{\tilde{\Theta}} \in \mathcal{L}_\infty$;
3. and, $K_\gamma \tilde{\gamma} + K_\alpha \tilde{\alpha} + K_Q \tilde{Q}$ is s^2 -small in the mean squared sense with s^2 is defined in (11);

where $(\tilde{\gamma}, \tilde{\alpha}, \tilde{Q}) = (\gamma - \gamma_c, \alpha - \alpha_c, Q - Q_c)$ and $\Theta = [\Theta_L, \Theta_{L_\alpha}, \Theta_M]$, for $i = 1, \dots, m$. All other symbols are defined in the appendix.

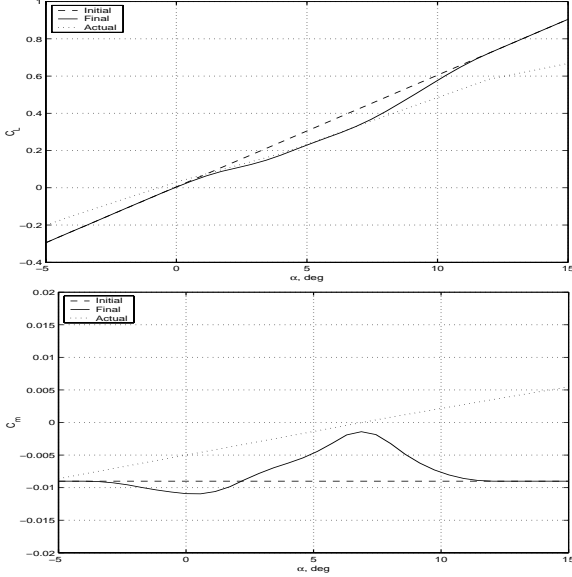


Figure 1: Plots of the actual aerodynamic functions $C_{M_o}(x_r)$ and $C_{L_o}(x_r) + C_{L_\alpha}(x_r)\alpha$ versus alpha. The approximations to these functions at the beginning and end of the simulation are also shown.

3 Simulation Analysis

The preceding sections have presented the theory for the design of an approximation based back-stepping controller. This section presents simulation results for the controller summarized in Table 1. The controller parameters are $K_\gamma = 0.3$, $K_\alpha = 3$, $K_Q = 30$, $\nu_\gamma = -(10\tilde{\gamma})^3$, $\nu_\alpha = -(10\tilde{\alpha})^3$, and $\nu_Q = 0$ where $\tilde{\gamma}$ and $\tilde{\alpha}$ are in radians. The vehicle for these simulations is a tailless uninhabited combat air vehicle (UCAV) with one engine and six control surfaces (i.e., $\delta_1 =$ right outer flap, $\delta_2 =$ left outer flap, $\delta_3 =$ right mid flap, $\delta_4 =$ left mid flap, $\delta_5 =$ right spoiler, and $\delta_6 =$ left spoiler). The spoilers are directly in front of the mid-flaps. Therefore, the midflap effectiveness is a function of the spoiler deflection. The spoiler deflection is restricted to be positive. The nonlinear aircraft simulation incorporates second order actuator models with magnitude and rate limit constraints. The thrust has first order, rate limited dynamics, with magnitude limited to the range [100,5000] lbs. When the thrust command is below its lower limit, the spoilers are deflected to create the necessary drag to cause the vehicle to track the commanded speed. The open loop vehicle is unstable.

As summarized in the right column of Table 1, 10 functions will be approximated. For all functions except $C_{M_{\delta_3}}$ and $C_{M_{\delta_4}}$, the regressor argument is $x_r = (\alpha, M)$. For $C_{M_{\delta_3}}$, the regressor argument is $x_r = (\alpha, M, \delta_5)$. For $C_{M_{\delta_4}}$, the regressor argument is $x_r = (\alpha, M, \delta_6)$. Each element of the regressor vector $\phi(x_r)$ is currently implemented as third order B-spline. The spline and

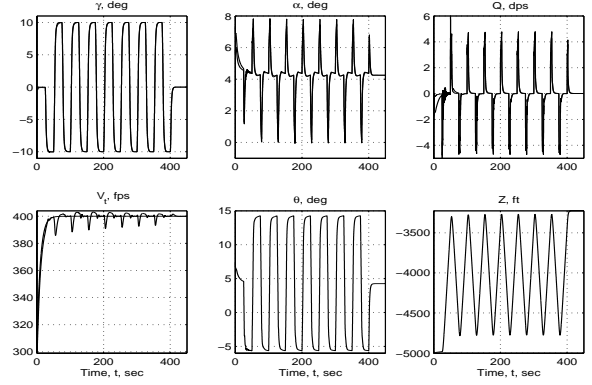


Figure 2: Time series plots of the longitudinal actual and commanded states of the aircraft (two plots per graph). The simulation starts with all coefficients of the aerodynamics model incorrect. The vehicle is commanded to fly at 400 fps and execute a series of 10 degree γ doublets.

on-line approximation implementation are designed so that significantly fewer than N regressor elements and model parameters are computed at each iteration (see [9]). The spline knots for α are spaced every 2 degrees between -8 and 20 degrees. The spline knots for M are spaced every 0.2 units between 0.0 and 1.0. The spline knots for spoiler deflection are spaced every 10 degrees between 0.0 and 60.

At $t=0$, the vehicle is flying $V=300$ fps with an altitude of 5000 ft, when an event occurs that changes the aircraft dynamics. Therefore, all of the aerodynamic coefficient functions in the controller become incorrect. For example, Figure 1 shows the actual coefficient of lift and coefficient of moment functions compared to the controller approximations to the same functions at the start and end of the simulation. The commanded and actual state trajectories are shown in Figure 2 for the subsequent 450 s. During this period of time, the vehicle speed is commanded to 400 fps, and starting at $t=25$ s the γ command is a series of 10 degree doublets with a period of 50 seconds. The γ doublets are pre-filtered by a first order filter with a pole at $s=-0.5$ and a 5 degree per second rate limit. This prefilter provides $\dot{\gamma}_c$ and a continuous γ_c . The α_c and Q_c signals are generated within the control law according to eqns. (4-5). The actuator signals are displayed in Fig. 3(a). The time series for the tracking errors are shown in Fig. 3(b). To more easily compare the tracking errors for repetitions of the same portion of the command, Fig. 3(c) displays the first 20 seconds of the tracking errors following $t = 50, 150, 250,$ and 350 s. At each of these times, the signal γ_c has just switched from -10 to 10 deg. Note that the tracking errors are small, converge toward zero during each doublet, and the peak errors between repetitions of doublets is decreasing. Also, the energy

(i.e., integrated squared error) of each tracking error appears to decrease from one repetition of the doublet to the next. The tracking errors for the same initial condition and command sequence, but with the parameter adaptation turned off is shown in Figure 3(d). Note that even without on-line approximation, the tracking errors of the controller are bounded; however, the bound is significantly larger.

Figure 1 shows the initial and final approximations to $C_{M_o}(x_r)$ and $C_{L_o}(x_r) + C_{L_\alpha}(x_r)\alpha$ along with the actual functions. The graphs are only shown as a function of α , but the regressor input x_r is multi-dimensional as described above. Note that the approximations converge toward the actual functions for $\alpha \in [3, 10]$ which is the region of the operating envelope about which the vehicle has operated during the duration of this 450 s simulation. Note that convergence of the approximated functions is *not* required for the tracking errors to behave well. The approximated functions can be forced to converge, if desired, by adding additional excitation (either by changing the γ_c signal or by altering the actuator signals within the null space of the G_Q matrix).

4 Issues and Conclusions

This article has presented design, analysis, and simulation results for a backstepping controller incorporating on-line approximation of the aerodynamic coefficients as functions over the operating envelope. Several previous results in the literature have presented controllers incorporating on-line adaptation of linearized aerodynamic coefficients; however, since the optimal linearized aerodynamic coefficients change with operating point, such linear adaptive methods may have significant transients when the flight conditions change. Those transients would re-occur as the aircraft cycled through a set of operating points, since such linear adaptive approaches are incapable of storing model information as a function of operating point. On-line approximation of the aerodynamic coefficients as a function over the operating envelope is a form of spatial memory, each time the aircraft enters a new region of the operating envelope, the model parameters that the controller uses are the last parameters that it had previously estimated while in that region. At the initiation of the controller, prior knowledge about the approximated functions can be used, either by initializing the approximator parameter vectors or by additive known functions. While prior initialization is not required, it will improve the initial transient performance.

The main focus of this article is not actuator distribution. The simulation results presented herein used pseudo-inverse based control distribution, but the stability results are not dependent on that actuator distribution approach. Although various other actuator distribution approaches are available, two points are important and will occur with any actuator distribution

approach. The first potential issue is that the estimated G_Q matrix may lose full row rank even while the actual G_Q matrix still has full row rank. This issue did not occur in our simulation results, but would need to be addressed in a flight ready control approach. If the designer can define a convex set \mathcal{S} (e.g., each element of \hat{G}_Q having an *a priori* fixed sign) which is known to contain the true control effectiveness parameters and which ensures the full row rank of \hat{G}_Q , then projection methods can be used to avoid this condition. Alternatively, since it is assumed that the actual vehicle is controllable throughout the operating envelope \mathcal{D} , it is possible to monitor the condition of $\hat{G}_Q \hat{G}_Q^T$. If this matrix approaches singularity, then the actuator distribution algorithm can use the actuator effectiveness matrix null space to enhance the ability to estimate the actuator effectiveness parameters. The second potential issue is actuator saturation. The actuator distribution algorithm can use the null space of \hat{G}_Q to achieve u_Q even though some of the actuators may be at a saturation limit. When it is not possible to achieve u_Q due to actuator saturation, non-zero tracking error will occur that is caused by saturation, not by model error; therefore, the on-line approximation approach will require modification. One approach that will work is to stop the parameter adaptation when u_Q is not being achieved due to actuator saturation. A more subtle approach that allows on-line approximation to continue even during saturation is being developed as a current research project.

5 Acknowledgements

This research supported by Barron Corporation through Air Force PRDA 01-03-VAK, University of California–Riverside, and University of Cincinnati.

References

- [1] M. Azam and S. N. Singh, “Invertibility and Trajectory Control for Nonlinear Maneuvers of Aircraft,” *J. of Guid., Cont., and Dyn.*, 17(1): 192–200, 1994.
- [2] M. A. Khan and Ping Lu, “New Technique for Nonlinear Control of Aircraft,” *J. of Guid., Cont., and Dyn.*, 17(5): 1055–1060, 1994.
- [3] J. G. Batterson and V. Klein, “Partitioning of Flight Data for Aerodynamic Modeling of Aircraft at High Angles of Attack,” *J. of Aircraft*, 26(4): 334–339, 1989.
- [4] J. S. Brinker and K. A. Wise, “Flight Testing of a Reconfigurable Control Law on the X-36 Tailless Aircraft,” *J. of Guid., Cont., and Dyn.*, 24(5): 903–909, 2001.
- [5] D. Bugajski, D. F. Enns, M. Elgersma, “A Dynamic Inversion Based Control Law with Appl. to High Angle of Attack Research Vehicle,” *AIAA-90-3407-CP*, pp. 826–839.
- [6] A. J. Calise, R. T. Rysdyk, “Nonlinear Adaptive Flight Control using Neural Networks,” *IEEE Control Systems Magazine*, pp. 14–25, 1998.
- [7] A. J. Calise, S. Lee, M. Sharma, “Development of a

Reconfigurable Flight Control Law for the X-36 Tailless Aircraft,” in J. of Guid., Cont., and Dyn., 24(5): 896-902, 2001.

[8] J. Y. Choi and J. A. Farrell, “Nonlinear Adaptive Control Using Networks of Piecewise Linear Approximators,” IEEE Trans. on Neural Networks, 11(2):390-401, 2000.

[9] Farrell, J., “Stability and Approximator Convergence in Nonparametric Nonlinear Adaptive Control”. IEEE Trans. on Neural Networks, Vol. 9(5): 1008–1020, 1998.

[10] W. L. Gerrard, D. F. Enns, and A. Snell, “Nonlinear Longitudinal Control of a Supermaneuverable Aircraft,” 1989 ACC, pp. 142–147, 1989.

[11] S. H. Lane and R. F. Stengel, “Flight Control Design Using Nonlinear Inverse Dynamics,” Automatica, 31(4): 781-806, 1988.

[12] M. Krstić, I. Kanellakopoulos, and P. Kokotović, Nonl. and Adapt. Cont. Design, John Wiley, 1995.

[13] P. K. A. Menon, M. E. Badget, R. A. Walker, and E. L. Duke, “Nonlinear Flight Test Trajectory Controllers for Aircraft,” J. of Guid., Cont., and Dyn., 10(1): 67–72, 1987.

[14] G. Meyer, R. Su, and L. R. Hunt, “Application of Nonlinear Transformations to Automatic Flight Control,” Automatica, 20(1): 103-107, 1984.

[15] M. M. Polycarpou, “Stable Adaptive Neural Control Scheme for Nonlinear Systems,” IEEE Trans. on Automatic Control, 41(3): 447-451, 1996.

[16] M. Polycarpou and M. Mears, “Stable Adaptive Tracking of Uncertain Systems Using Nonlinearly Parametrized On-Line Approximators,” Int. J. of Control, 70(3): 363–384, 1998.

[17] R. T. Rysdyk, Adaptive Nonlinear Flight Control, Ph.D. Thesis, Georgia Institute of Technology, School of Aero. Eng., Atlanta, GA, 1998.

[18] S. N. Singh and M. Steinberg, “Adaptive Control of Feedback Linearizable Nonlinear Systems with Application to Flight Control,” J. of Guid, Control, and Dynamics, 19(4): 871–877, 1996.

[19] S. A. Snell, D. F. Enns, and W. L. Garrard Jr., “Nonlinear Inversion Flight Control for a Supermaneuverable Aircraft,” J. of Guid., Cont., and Dyn., 14(4): 976–984, 1992.

[20] M. Sharma, A. J. Calise, and J.E. Corban, “Application of an Adaptive Autopilot Design to a Family of Guided Munitions,” AIAA GNC Conf., AIAA-2000-3969.

[21] M. Steinberg and A. Page, “Nonlinear Adaptive Flight Control with Genetic Algorithm Design Optimization,” Int. J. of Rob. and Nonl. Cont., 9: 1097-1115, 1999.

[22] B. L. Stevens and F. L. Lewis, “Aircraft Control and Simulation,” John Wiley, 1992.

[23] T. L. Trankle and S. D. Bachner, “Identification of a Nonlinear Aerodynamic Model of the F-14 Aircraft,” J. of Guid., Cont., and Dyn., 18(6): 1292-1297, 1995.

[24] T. L. Trankle, J. H. Vincent, and S. N. Franklin, “System Identification of Nonlinear Aerodynamic Models,” Adv. in the Techniques and Technology of the Appl. of Nonlinear Filters and Kalman Filters, AGARDograph No. 256, 1982.

[25] D. Ward, J. Monaco, R. Barron, and R. Bird, “Self-Designing Controller: Design, Simulation, and Flight Test Evaluation,” WL-TR-97-3095, 1996.

A Reduced Longitudinal Dynamic Model

For $R = P = \phi = \beta = 0$, the aircraft dynamics are

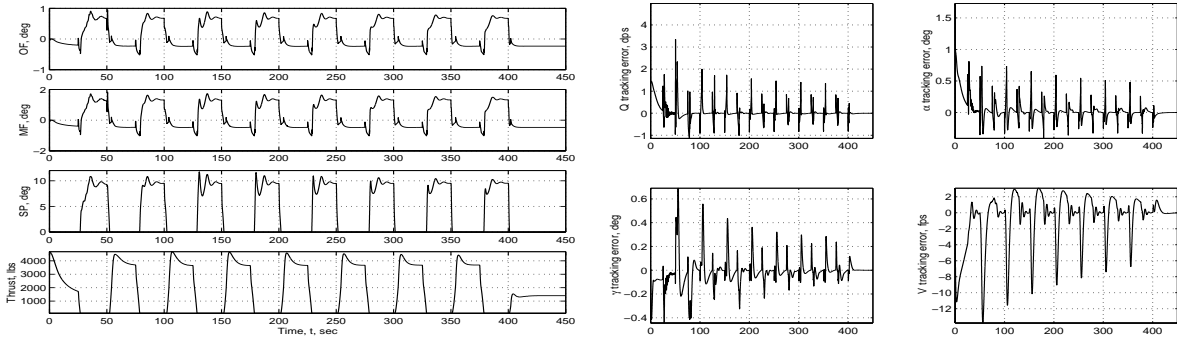
$$\begin{aligned}\dot{V} &= \frac{1}{m}[T \cos(\alpha) - D - m g_o \sin(\theta - \alpha)] \\ \dot{\alpha} &= \frac{1}{mV}[-T \sin(\alpha) - L + mVQ + m g_o \cos(\theta - \alpha)] \\ \dot{Q} &= c_7 \bar{M} + f_Q \\ \dot{\theta} &= Q\end{aligned}$$

where the various symbols are defined below [22].

Symbol	Meaning
α	Angle of attack
α_c	Commanded Angle of attack
$\tilde{\alpha}$	Angle of attack tracking error
\bar{c}	Mean aerodynamic chord
$c_i, i \in [1, 9]$	Inertial parameters (see p.80 in [22])
$C_D(x_r)$	Coefficient of drag
$C_L(x_r)$	Coefficient of lift
$C_{L\alpha}(x_r)$	Coefficient of lift with respect to α
$C_{M_o}(x_r)$	Coefficient of pitch moment
$C_{M_Q}(x_r)$	Coefficient of pitch moment due to Q
$C_{M_{\delta_i}}(x_r)$	Coefficient of pitch moment due to deflection of surface i
δ^T	The vector of control surface deflections
$D(x)$	Drag force function
$\hat{D}(x_r)$	Approximated drag force function
γ	Flight path angle
γ_c	Commanded flight path angle
$\tilde{\gamma}$	Flight path angle tracking error
g	gravity
K_Q	Control parameter for Q loop
K_α	Control parameter for α loop
K_γ	Control parameter for γ loop
$L(x)$	Lift force function
$\hat{L}(x_r)$	Approximated lift force function
m	Number of control surfaces
M	Mach number
$\bar{M}(x)$	Pitch moment function
$\hat{\bar{M}}(x_r)$	Approximated pitch moment function
$\phi(x_r)$	Regressor vector
\bar{q}	Dynamic pressure
Q	Pitch rate
Q_c	Commanded pitch rate
\tilde{Q}	Pitch rate tracking error
ρ	Air density
S	Reference surface area
T	Thrust
θ	Pitch Angle
V	Airspeed
V_c	Commanded airspeed
\tilde{V}	velocity tracking error
x	Vehicle state vector
x_r	Reduced state vector containing only the dominant elements.

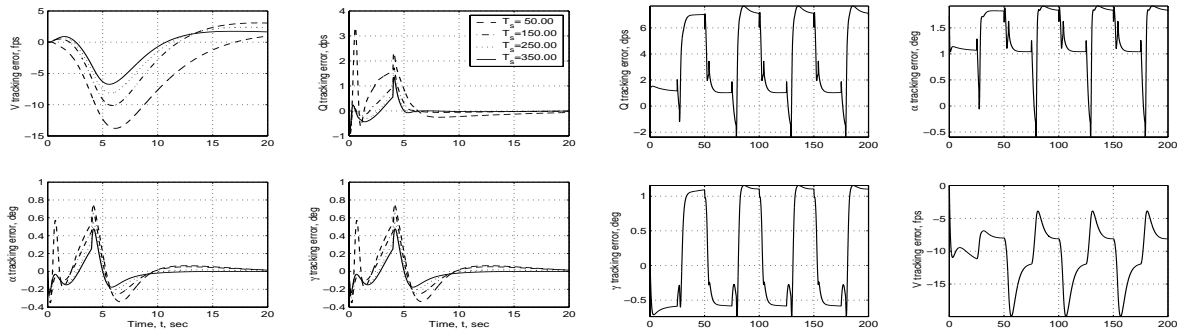
$\alpha_c = \frac{1}{\hat{C}_{L\alpha}} \left(-\hat{C}_L + \frac{mV}{\bar{q}S} (-f_\gamma + \dot{\gamma}_c - K_\gamma \tilde{\gamma} + \nu_\gamma) \right)$	$\hat{C}_{L_o} = \Theta_{L_o}^T \phi(x_r)$
$Q_c = \frac{\bar{q}S(\hat{C}_L + \hat{C}_{L\alpha}\alpha)}{mV} - K_\alpha \tilde{\alpha} + f_\gamma + \dot{\alpha}_c + \nu_\alpha - \tilde{\gamma} \frac{\bar{q}S\hat{C}_{L\alpha}}{mV}$	$\hat{C}_{L\alpha} = \Theta_{L\alpha}^T \phi(x_r)$
$u_Q = -\bar{q}S\bar{c} \left(\hat{C}_{M_o}(x_r) + \hat{C}_{M_Q}(x_r) \frac{\bar{c}Q}{2V} \right) + \frac{1}{c_7} \left(-K_Q \tilde{Q} + \dot{Q}_c + \nu_Q - \tilde{\alpha} - f_Q \right)$	$\hat{C}_{M_o} = \theta_{M_o}^T \phi(x_r)$
$\delta = d + W^{-1} \hat{G}_Q^T \left[\hat{G}_Q W^{-1} \hat{G}_Q^T \right]^{-1} \left(u_Q - \hat{G}_Q d \right)$	$\hat{C}_{M_Q} = \Theta_{M_Q}^T \phi(x_r)$
$\hat{G}_Q = \bar{q}S\bar{c} \left[\hat{C}_{M_{\delta_1}}, \dots, \hat{C}_{M_{\delta_m}} \right]^T$	$\hat{C}_{M_{\delta_i}} = \Theta_{M_{\delta_i}}^T \phi(x_r)$

Table 1: On-line approximation based (γ, α, Q) controller summary including pseudoinverse based control surface allocation. The parameter adaptation equations are specified in eqns. (6–7) and (8–10). The matrix W is positive definite and the index $i \in [1, m]$.



(a) Plots of the surface positions and thrust commands required to execute the state trajectory displayed in Fig. 2.

(b) Time series of the command tracking errors for the longitudinal states.



(c) First twenty seconds of transients to γ commands starting at $t = 50, 150, 250,$ and 350 s.

(d) Time series of the command tracking errors for the longitudinal states for the backstepping controller with the parameter adaptation turned off.

Figure 3: Simulation results.